On the Estimation Algorithm Used in Adaptive Performance Optimization of Turbofan Engines

Martín D. España and Glenn B. Gilyard

December 1993

NASA Technical Memorandum 4551

On the Estimation Algorithm Used in Adaptive Performance Optimization of Turbofan Engines

Martín D. España and Glenn B. Gilyard
Dryden Flight Research Facility
Edwards, California

ABSTRACT

The performance seeking control algorithm is designed to continuously optimize the performance of propulsion systems. The performance seeking control algorithm uses a nominal model of the propulsion system and estimates, in flight, the engine deviation parameters characterizing the engine deviations with respect to nominal conditions. In practice, because of measurement biases and/or model uncertainties, the estimated engine deviation parameters may not reflect the engine's actual off-nominal condition. This factor has a necessary impact on the overall performance seeking control scheme exacerbated by the open-loop character of the algorithm. In this report, the effects produced by unknown measurement biases over the estimation algorithm are evaluated. This evaluation allows for identification of the most critical measurements for application of the performance seeking control algorithm to an F100 engine. An equivalence relation between the biases and engine deviation parameters stems from an observability study; therefore, it is undecided whether the estimated engine deviation parameters represent the actual engine deviation or whether they simply reflect the measurement biases. A new algorithm, based on the engine's (steady-state) optimization model, is proposed and tested with flight data. When compared with previous Kalman filter schemes, based on local engine dynamic models, the new algorithm is easier to design and tune and it reduces the computational burden of the onboard computer.

NOMENCLATURE

$\mathbf{A}, \mathbf{B}, \mathbf{C}, \mathbf{D}, \mathbf{L}, \mathbf{M}$	state variable model matrices
$AAHT$	area adder high-pressure turbine deviation parameter, in^2
AJ	nozzle throat area, in^2
BLD	bleed airflow, lb/sec
CEM	compact engine model
CIM	compact inlet model
$CIVV$	compressor inlet variable guide vane angle, deg
CPSM	compact propulsion system model
DEEC	digital electronic engine control
$DEHPT$	high-pressure turbine efficiency deviation parameter, percent
$DELPT$	low-pressure turbine efficiency deviation parameter, percent
$DINL$	inlet drag, lbf
$DWFAN$	fan airflow component deviation parameter, lb/sec
$DWHPC$	high-pressure compressor airflow deviation parameter, lb/sec
EDP	engine deviation parameter
F	matrix
$FTIT$	fan turbine inlet temperature, °F
f	function
$\mathbf{G}_y, \mathbf{G}_{aux}, \mathbf{H}_y, \mathbf{H}_{aux}$	gain submatrices of the optimization model
HPX	power extraction, hp
h	function

$\mathbf{I}_m$	identity matrix of dimension m
KF	Kalman filter
$\mathbf{K_x, K}_\eta$	respectively, $\mathbf{x}$ and η columns of the steady-state Kalman filter gain
lim	limit
M	Mach number
m	dimension of $\mathbf{y}$
$N1$	fan rotor speed, rpm
$N2$	compressor rotor speed, rpm
n	dimension of $\mathbf{x}$
$\mathbf{P, Q, R}$	respectively: estimate, process, and measurement covariance matrices
P_{amb}	ambient pressure, lb/in^2
PB	burner pressure, lb/in^2
PSC	performance seeking control
$PS2$	static pressure at engine face, lb/in^2
PT	total pressure, lb/in^2
p	dimension of η
$RCVV$	rear compressor variable vanes, deg
SOAPP	state of the art propulsion program
SSMLO	steady-state model-based Luenberger observer
SSVM	steady-state variable model
SVM	state variable model
TMT	composite turbine metal temperature, °F
TSFC	thrust-specific fuel consumption
TT	total temperature, °F
t	time, sec
$\mathbf{U, u}$	respectively, input vector and incremental input vector
$V(p)$	a neighborhood of the point p
$WCFAN$	corrected fan airflow, lb/sec
$WCHPC$	corrected high-pressure compressor airflow, lb/sec
WF	gas generator fuel flow, lb/hr
$\mathbf{x}$	incremental state vector
$\mathbf{Y, y}$	respectively, measured and incremental measured output vector
$\mathbf{Y}_{aux}, \mathbf{y}_{aux}$	respectively, unmeasured and incremental unmeasured output vectors
$\mathbf{Z, z}$	respectively, output vector and incremental output vector
γ, ν	respectively, bias vector in the output and input measurements
δ	increment operator
η	engine deviation parameters vector
ξ	state vector
λ, Λ	respectively, vector of eigenvalues and eigenvalues diagonal matrix

2

$(\omega_x, \omega_\eta), \rho$ respectively, process and measurement noise of the Kalman filter model

Subscripts

aux	auxiliary
b	base point
eq	equivalent

Suffix, PW1128 engine station numbers, figure 1

2	fan inlet
2.5	compressor inlet
3	compressor discharge
4	high-pressure turbine inlet
4.5	low-pressure turbine inlet
6	afterburner inlet
7	nozzle throat

Symbols

$E\{\}$	expected value operator
$\mathbb{R}$	the set of real numbers
$\in$	is a member of
$\otimes$	tensor product
$\cdot$	time derivative operator
$[\ ]^T$	matrix transpose
$\hat{\ }$	estimated variable
$\tilde{\ }$	estimation error
$\underset{=}{\triangle}$	equals by definition

INTRODUCTION

Personnel from the NASA Dryden Flight Research Facility (Edwards, California), the McDonnell Douglas Corp. (St. Louis, Missouri), and United Technologies Pratt & Whitney (West Palm Beach, Florida) have developed a control strategy allowing to operate a turbofan engine-based propulsion system as closely as possible to its optimum steady-state working condition without compromising reliability and operability. The resulting control strategy is called performance seeking control (PSC) (refs. 1–4). Three different operating modes are sought corresponding, respectively, to three different optimization criteria. They are: (1) minimum fuel consumption, (2) minimum temperature of the hot section of the engine (also called extended engine life mode, given the influence of high temperatures on the life of the engine), and (3) maximum thrust.

3

The optimization is based on a steady-state model of the entire propulsion system (integrating the inlet, the engine, and the nozzle), called the optimization model. A fixed model of the propulsion system would not be able to account for the significant changes experienced by the engine during its life span (engine deterioration) or for the differences from aircraft to aircraft resulting from manufacturing variability. As such, a mechanism for the adaptation of the engine model is required. For this purpose, the current engine operating condition is characterized by a set of adjustable parameters, called the engine deviation parameters (EDPs), which are included in the optimization model. The EDPs are estimated in flight and their estimates are introduced into the optimization process/model—this fact gives the PSC system an adaptive character. The estimation is performed with a Kalman filter (KF) based on a reduced-order linear dynamic model of the engine called the estimation model.

The PSC system testing at subsonic flight conditions (ref. 2) was recently concluded for the F100 (Pratt & Whitney) engine-based F-15 (McDonnell Douglas) propulsion system. The results show up to 15-percent increases in thrust, up to 100 °R reductions in the turbine temperature, and between 1- and 2-percent savings in thrust-specific fuel consumption (TSFC). Preliminary flight evaluations of the PSC algorithm at supersonic flight conditions have been performed indicating thrust increases of approximately 10 percent and a TSFC reduction of approximately 9 percent (ref. 5).

The algorithm is expected to work well when the estimated values of the EDPs actually represent the current off-nominal conditions of the engine. However, it has been shown during flight testing (ref. 2) that the estimated EDPs may not correspond to known levels of engine deterioration. This fact is attributed to other sources of model–engine mismatch not accounted for by the EDPs. Poor EDP estimates translate into an inadequate prediction (provided by the optimization model) of the engine's behavior, which in turn may degrade the optimization process. Given the importance of the estimation algorithm in the overall adaptive PSC scheme, additional research is key for evaluating the effects of model inaccuracies and measurement biases over the optimization process, or for developing new algorithms which are less model-dependent.

In this paper we show first that, with the present measurement system, unknown biases cannot be estimated independently of the EDPs and consequently, there may not be compensation for their effects. A sensitivity approach is proposed to quantify the biases' influence over the predictions of the steady-state optimization model. The study allows us to decide, for the F100 engine, which measurement biases have more influence over the estimation process and which estimates are affected the most by the biases.

We next propose a Luenberger-type estimation algorithm based on the same (steady-state) model used by the optimization process. Compared to the presently used KF approach, the new algorithm yields estimates of a similar quality, but has a reduced complexity, requires considerably fewer computer resources, and is easier to tune. The proposed steady-state model based Luenberger observer (SSMLO) and the KF are compared using flight data from an F-15 propulsion system.

4

BACKGROUND AND PROBLEM FORMULATION

The PSC system was implemented on the NASA F-15 research airplane, which is powered by two F100 derivative (PW1128) afterburning turbofan engines system (ref. 2). The aircraft was modified with a full-authority digital electronic engine control (DEEC) system. The DEEC system provides basic open-loop scheduling and closed-loop feedback control of the propulsion variables (ref. 2). Its software was modified to accommodate PSC trim commands without altering the basic control functions. Figure 1 is an F100 engine diagram showing the location of the DEEC instrumentation, the DEEC-calculated variables, and the parameters calculated by the PSC algorithm. Figure 2 shows the flow of the information within the PSC algorithm. The PSC algorithm essentially consists of an estimation algorithm to update the EDPs' estimates and an open-loop optimization control law based on a set of local models of the propulsion system. The current local model is selected based on flight data. More details of the overall structure of the PSC system can be found in reference 2.

The engine model relates the input vector $\mathbf{U}$ with the output vector $\mathbf{Z}$ defined as:

$$\mathbf{U}^T \triangleq [WF\ AJ\ CIVV\ RCVV\ HPX\ BLD] \tag{1a}$$

$$\mathbf{Z}^T \triangleq \left[\mathbf{Y}^T, \mathbf{Y}_{aux}^T\right] \tag{1b}$$

where:

$$\mathbf{Y}^T \triangleq [N1\ N2\ PT4^*\ FTIT\ PT6] \tag{1c}$$

$$\mathbf{Y}_{aux}^T \triangleq [TT6\ WCFAN\ PT2.5\ TT2.5\ TT3\ TT4\ WCHPC] \tag{1d}$$

$\mathbf{Y}$ represents the measured components of $\mathbf{Z}$. The unmeasured vector $\mathbf{Y}_{aux}$, called the auxiliary variables vector, is calculated within the optimization process of the PSC algorthim.

The engine model is the most variable of the three main components of the propulsion system, i.e., the inlet, the engine, and the nozzle. Consistently, the propulsion model uncertainties are assumed to be concentrated in the engine. Five coefficients of the aerothermodynamic equations of the engine have been selected as quantifiers of the engine's off-nominal behavior (or engine–model mismatch). The deviations of these coefficients with respect to their nominal values are called the EDPs and are denoted as (refs. 1–4):

$$\eta^T \triangleq [DEHPT\ DELPT\ DWHPC\ DWFAN\ AAHT] \tag{2}$$

The components of η correspond to deviations, respectively, in: the efficiencies in the low- and high-pressure turbines ($DELPT$ and $DEHPT$); the airflow in the fan and high-pressure compressor ($DWFAN$ and $DWHPC$), and the effective high-pressure turbine area ($AAHT$). For the nominal engine, $\eta = 0$.

$^*PT4$ is considered as a measured variable even though it is calculated as function of the measure of PB.

We now define:

$$\mathbf{u} \triangleq \mathbf{U} - \mathbf{U}_b; \quad \mathbf{y} \triangleq \mathbf{Y} - \mathbf{Y}_b; \quad \mathbf{z} \triangleq \mathbf{Z} - \mathbf{Z}_b \tag{3}$$

where $\mathbf{U}_b$, $\mathbf{Y}_b$, and $\mathbf{Z}_b$ are, respectively, the vectors $\mathbf{U}$, $\mathbf{Y}$, and $\mathbf{Z}$ evaluated at some predicted engine trim point called a base point.

The following linear model has been used (ref. 1) to characterize, locally around a base point, the dynamic relationship between the input $\mathbf{U}$ and the measured output $\mathbf{Y}$ for a given off-nominal condition quantified by the time-invariant vector η.

$$\dot{\mathbf{x}} = \mathbf{Ax} + \mathbf{Bu} + \mathbf{L}\eta \tag{4a}$$

$$\dot{\eta} = 0 \tag{4b}$$

$$\mathbf{y} = \mathbf{Cx} + \mathbf{Du} + \mathbf{M}\eta \tag{4c}$$

Equations (4a, b, and c) are called the state variable model (SVM). The incremental state variable $\mathbf{x}$ is defined as:

$$\mathbf{x}^T \triangleq [N1 - N1_b, \ N2 - N2_b, \ TMT - TMT_b] \tag{5}$$

where, TMT, called the turbine metal temperature, is a composite variable representing the thermal state of the hot section of the engine. Again, $N1_b$, $N2_b$ and TMT_b represent the corresponding variables at the base point. Finally, $\mathbf{A}$, $\mathbf{B}$, $\mathbf{C}$, $\mathbf{D}$, $\mathbf{L}$, and $\mathbf{M}$ are matrices with the appropriate dimensions.

The continuum set of possible base points covering the operation range of a nominal engine for a particular reference flight condition is discretized. The discrete base points are indexed with the variables $PT6$ and $PT4$ and computed using a detailed model of the whole propulsion system, called the state of the art propulsion program (SOAPP) (ref. 6). The matrices $\mathbf{A}$ to $\mathbf{M}$ in equations (4a, b, and c) are calculated by numeric linearization, using the SOAPP for a set of 49 base points covering the power-setting range and indexed with $PT4$ ranging over the interval 23 to 260 lb/in^2. The matrices are updated in flight, based on the $PT4$ index nearest to the current value of $PT4$ with some hysteresis to avoid undesired switching. The reference flight condition corresponds to standard day conditions, Mach 0.9, and an altitude of 30,000 ft. By using correction factors, calculated as a function of the total inlet pressure and temperature, the results can be converted to the actual given flight conditions. In this way, the validity of the model can be extended to the whole flight envelope.

Estimation Process of the PSC Algorithm

The vector η is presently estimated using a Kalman filter (KF) based on the following modification of the engine's piecewise dynamic linear model given by equations (4a, b, and c) (refs. 1, 4).

$$\dot{\mathbf{x}} = \mathbf{Ax} + \mathbf{Bu} + \mathbf{M}\eta + \omega_x \tag{6a}$$

$$\dot{\eta} = \omega_\eta \tag{6b}$$

$$\mathbf{y} = \mathbf{Cx} + \mathbf{Du} + \mathbf{M}\eta + \rho \tag{6c}$$

ω_η, ω_x, and ρ are centered white noises with positive definite covariance matrices, respectively: Q_η, Q_x, and R. We shall also need the definition:

$$Q \triangleq \begin{bmatrix} Q_x & 0 \\ 0 & Q_\eta \end{bmatrix}$$

With the previous assumptions, η is estimated, together with x using the asymptotic KF:

$$\begin{bmatrix} \dot{\hat{x}} \\ \dot{\hat{\eta}} \end{bmatrix} = F \begin{bmatrix} \hat{x} \\ \hat{\eta} \end{bmatrix} + Gu + K \left(y - H \begin{bmatrix} \hat{x} \\ \hat{\eta} \end{bmatrix} \right) \tag{7}$$

where (see, for instance refs. 7 or 8):

$$F \triangleq \begin{bmatrix} A & L \\ 0 & 0 \end{bmatrix}; \quad G \triangleq \begin{bmatrix} B \\ 0 \end{bmatrix}; \quad H \triangleq [C : M]; \quad K \triangleq \begin{bmatrix} K_x \\ K_\eta \end{bmatrix} = PH^T R^{-1} \tag{8}$$

P is the steady-state solution of the Riccati (ref. 8) differential equation associated to the covariance matrix of the estimates and can be calculated from:

$$FP + PF^T + Q - PH^T R^{-1} HP = 0 \tag{9}$$

R is estimated from the sample statistics of the output measurements. The submatrix Q_x can be associated with the input noise. The submatrix Q_η has no physical meaning in this context. However, as can be shown from equations (8) and (9) and straightforward calculations, if Q_η is assumed to be zero, the submatrix K_η of the steady-state gain K in equation (7) is also zero, thus preventing the realization of the filter*. In practice, the entries of Q_η are used as "tuning parameters" empirically adjusted so as to give a good compromise between time response and noise rejection. The design gives as a result 49 matrices $K \in \mathbb{R}^{8 \times 5}$ (one for each point indexed by $PT4$) that are stored together with the matrices A to M.

Remark Because of the artificial introduction of the matrix Q_η, no claim can be made concerning the optimality of the resulting filter. Furthermore, as can be seen from equations (7), (8), and (9), the filter's eigenvalues (those of the matrix $F - KH$) do not have a simple relationship with the tuning parameters (entries of the matrix Q_η). This complicates the tuning of the filter's dynamic response, which can only be done after extensive simulations.

A new estimation scheme based on the engines steady-state optimization model, is proposed in this report. Compared with the KF approach, the new estimator is easier to design and tune. Furthermore, the new scheme considerably reduces the computational burden.

Optimization Model of the PSC Algorithm

The optimization model of the PSC algorithm (see fig. 2) is a simplified steady-state model of the propulsion system called the compact propulsion system model (CPSM). It combines two submodels:

---

*This fact can be interpreted as follows: if η is an unknown time invariant random variable, the Kalman filter asymptotically estimates its exact value (with zero covariance). Thus, qualitatively speaking, when time goes to infinity, the filter "need not" incorporate any additional information about this variable from the measurements. Consequently, $K_\eta \longmapsto 0$.

the compact inlet model (CIM) and the compact engine model (CEM). The subsonic CIM calculates both the inlet drag ($DINL$) and the inlet pressure $PT2$ as functions of the Mach number, the corrected fan airflow ($WCFAN$), and the ambient pressure (P_{amb}). At subsonic flight the inlet geometry is scheduled and is not modified by the PSC algorithm. The CEM comprises the engine and the nozzle. Part of the CEM is the steady-state variable model (SSVM), which consists of a piecewise linearization of the steady-state formulation of the aerothermodynamic equations. Each of the SSVM's local models relates the vector η (defined in eq. (2)) with small increments of $\mathbf{Z}$, $\mathbf{Y}$, and $\mathbf{U}$ (see definitions in eqs. (3)) around a base point in the following way:

$$ \mathbf{z} = \begin{bmatrix} \mathbf{y} \\ \mathbf{y}_{aux} \end{bmatrix} = \begin{bmatrix} \mathbf{G_y} \\ \mathbf{G}_{aux} \end{bmatrix} \mathbf{u} + \begin{bmatrix} \mathbf{H_y} \\ \mathbf{H}_{aux} \end{bmatrix} \eta \tag{10} $$

where: $\mathbf{G_y} \in \mathbb{R}^{5\times6}$; $\mathbf{G}_{aux} \in \mathbb{R}^{7\times6}$; $\mathbf{H_y} \in \mathbb{R}^{5\times5}$; $\mathbf{H}_{aux} \in \mathbb{R}^{7\times5}$. The relationship between the incremental input vector $\mathbf{u}$ and the incremental measurable vector $\mathbf{y}$ can thus be written as:

$$ \mathbf{y} = \mathbf{G_y}\mathbf{u} + \mathbf{H_y}\eta \tag{11} $$

Equation (11) is the steady-state version of the SVM (eqs. (4)) and can be determined from the latter by equating the time derivatives to zero. Matrices $\mathbf{G_y}$, $\mathbf{G}_{aux}$, $\mathbf{H_y}$, and $\mathbf{H}_{aux}$ are calculated offline based on the SOAPP for each of the discrete tabulated base points. Their values are also tabulated and are used to determine, by interpolation, the current matrices of model (10) each time the base point is updated. The interpolation is performed using as indices the variables $PT4$ and $PT6$. By applying the *certainty equivalence principle* (see ref. 11), the last estimation of η is introduced into the model (10), which is used by the optimization process to determine the new trims to be sent to the actuators (see fig. 2). Notice that η is an intermediate entity used only to predict $\mathbf{z}$ for a given $\mathbf{u}$ inside the optimization process.

Effects of Other Sources of Model–Engine Mismatch

Some recent results show that there may be other off-nominal conditions not accounted for by the components of η. For instance, reference 4 shows, using flight data, that changes in the Reynolds index and biases in the measured variables have as a consequence that the estimated EDPs do not reflect known levels of engine degradation. In addition, model (4) may not represent the current linear tangent model of the engine; this factor can be caused by

1. The finite discretization of the space of local models.

2. Intermediate simplifications and order reduction of the engine's model before the determination of the linearized local models.

3. The neglected effects of the EDPs on the matrices $\mathbf{A}$, $\mathbf{B}$, $\mathbf{C}$, $\mathbf{D}$, $\mathbf{L}$, and $\mathbf{M}$ of the local dynamic models (4) or on the steady-state gain matrices of the SSVM (10) as seen in Appendix A.

In order to see how modeling errors affect the estimation process, let us consider the state estimation problem of the following generic linear system comparable with that of equations (4) (an explicit mention of the vector η or the inclusion of the matrices $\mathbf{M}$ and $\mathbf{L}$ is irrelevant here):

$$\dot{x} = Ax + Bu$$

$$y = Cx + Du \tag{12}$$

We next assume that the model used by the KF (corresponding to eq. (7)) is based on matrices A', B', C', D', which are different from the matrices of system (12).

$$\dot{\hat{x}} = A'\hat{x} + B'u + K(\hat{y} - y)$$

$$\hat{y} = C'\hat{x} + D'u \tag{13}$$

The estimation error equation is:

$$\dot{\tilde{x}} = (A' + KC')\tilde{x} + (\tilde{A} + K\tilde{C})x + (\tilde{B} + K\tilde{D})u \tag{14}$$

where the differences between the system's matrices and the model's matrices are denoted with a $\tilde{}$ (e.g. $\tilde{A} \triangleq A' - A$). For the u and x constant and $\tilde{A}$, $\tilde{B}$, $\tilde{C}$, or $\tilde{D}$ different from zero, (14) gives a steady-state estimation error $\tilde{x} \neq 0$ (= constant), which is proportional to the model matrices' inaccuracies weighted by the signals u and x.

Besides stating the importance of the model–engine mismatch in the estimation process we shall not further investigate its consequences but concentrate only on the biases' effects. When evaluating these effects one must take into consideration that for the PSC algorithm the primary objective is not an accurate estimation of η, but a reliable enough estimation of the (unmeasured) auxiliary variables of the optimization model (10). In this report we investigate those effects and determine, in the presence of unknown biases, which are the most critical measures in the PSC system, and, conversely, which are the most affected estimated auxiliary variables.

OBSERVABILITY CONDITIONS AND EQUIVALENCE BETWEEN BIASES AND EDPs

Observability of the EDPs

A necessary condition (see, for instance, ref. 8) for the existence of the asymptotic KF (eqs. (7) to (9)) is the *observability* of model (6) (consult ref. 9 for a definition of the notion of observability). Since the observability of model (6) can be tested directly from its matrices, the following question may be addressed: which is the largest dimension of η compatible with its identifiability? We prove that the dimension of η must be less than or equal to the number of available output measurements. For this, we use the following result proven in Appendix B.

Proposition 1 *If, given the model (4) (or (6)) with n the dimension of x, p the dimension of η, and m the dimension of y, the matrix:*

$$S = \begin{bmatrix} C & M \\ A & L \end{bmatrix} \tag{15}$$

is such that rank*(S) < n + p, then, model (4) (or (6)) is not observable.

Now, since **S** has at most rank $n + m$, a necessary condition for model (6) to be observable is that, according to Proposition 1, $n + m \geq n + p$ or, equivalently, $m \geq p$, which implies that **one needs at least as many measured outputs as the dimension of the vector** η. The latter condition is satisfied by the engine's model (4) or (6) with $p = m = 5$, implying that no extra estimable components can be added to the vector η to quantify an off-nominal engine condition, unless more measurements are made available.

Equivalence Between Biases and EDPs

Biases may be present either in the input or the output measured variables. With the present measurement system, the biases' effects cannot be distinguished from those produced by "equivalent" EDPs. This fact is shown as follows: consider the SVM (4) with an input bias vector ν and an output bias vector γ (some of the components of ν and γ may be zero).

$$\dot{x} = Ax + Bu + B\nu + L\eta, \quad x(0) = x^0 \tag{16a}$$

$$y = Cx + Du + D\nu + M\eta + \gamma \tag{16b}$$

$$\dot{\nu} = 0, \quad \dot{\eta} = 0, \quad \dot{\gamma} = 0 \tag{16c}$$

System (16) and the following:

$$\dot{\xi} = A\xi + Bu, \qquad \xi(0) = \xi^0 = x^0 - A^{-1}(B\nu + L\eta) \tag{17a}$$

$$y = C\xi + Du + (D - CA^{-1}B)\nu + (M - CA^{-1}L)\eta + \gamma \tag{17b}$$

$$\dot{\nu} = 0, \quad \dot{\eta} = 0, \quad \dot{\gamma} = 0 \tag{17c}$$

produce the same output given the same inputs and are thus indistinguishable from an input–output standpoint (they are input–output equivalent). In equations (17a, b, and c) the effects of biases and EDPs have all been referred to the output. By using the corresponding steady-state gain matrices of system (4), equation (17b) can also be written as: (see definition of H_y, G_y in eq. (11))

$$y = C\xi + Du + [H_y \; G_y \; I] \begin{bmatrix} \eta \\ \nu \\ \gamma \end{bmatrix} \tag{18}$$

From equation (18) and the equivalence between models (16) and (17), along with Proposition 1, one concludes that **the biases cannot be estimated unless more unbiased measures are made available**. Moreover, again from equation (18), one sees that the biases ν and γ cannot be distinguished from an (apparent) increment in η given by:

$$\eta_{eq} = H_y^{-1}(G_y\nu + \gamma) \tag{19}$$

The invertibility of the matrix H_y is clearly satisfied in practice, otherwise, it can be seen from equation (18) that the EDPs will not have independent effects on the measured outputs. Equation (19) explains how (and why) biases in measurements alter, in practice, the estimated EDPs. Moreover, it tells us that any off-nominal condition can be "simulated" by a particular set of measurement biases.

---

*The rank of a matrix being the number of its independent columns.

Estimation Errors Induced by the Biases

As shown previously, the effects of biases in the measurements cannot be distinguished from increments on the EDPs. Any estimation algorithm will then be unable to discern whether the apparent EDPs are the consequence of a real departure of the engine from its nominal behavior or whether they are simply caused by biases in the measurements. With the present measurement system the estimates are thus affected by an error that is impossible to determine unless the biases are known *a priori*. We now proceed to calculate the errors induced by the measurement biases.

We call $\eta_{eq}(\nu)$ and $\eta_{eq}(\gamma)$ the apparent increments of η (giving rise to a corresponding EDP estimation error) induced, respectively, by biases in the inputs and biases in the measured outputs. Now using equation (19), one has:

$$\eta_{eq}(\nu) = \mathbf{H_y}^{-1} \mathbf{G_y} \nu \tag{20}$$

$$\eta_{eq}(\gamma) = \mathbf{H_y}^{-1} \gamma \tag{21}$$

Since the estimation of η is affected by η_{eq}, the resulting estimate of $\mathbf{y}_{aux}$, obtained from model (10), is given by:

$$\hat{\mathbf{y}}_{aux} = \mathbf{G}_{aux}\mathbf{u} + \mathbf{H}_{aux}(\eta + \eta_{eq}(\nu) + \eta_{eq}(\gamma) + \tilde{\eta}) \tag{22}$$

where $\tilde{\eta}$ is the estimation error of $\hat{\eta}$ given by the KF. On the other hand, the actual (but unknown) value of $\mathbf{y}_{aux}$ is a function of the unknown bias ν and is given by:

$$\mathbf{y}_{aux} = \mathbf{G}_{aux}(\mathbf{u} + \nu) + \mathbf{H}_{aux}\eta \tag{23}$$

From equations (22) and (23), the estimation errors in the auxiliary variables induced, respectively, by the input biases and the output biases, are given by:

For the input bias case:

$$\tilde{\mathbf{y}}_{aux}(\nu) = \left[\mathbf{G}_{aux} - \mathbf{H}_{aux}\mathbf{H_y}^{-1}\mathbf{G_y} \right] \nu \tag{24}$$

For the output bias case:

$$\tilde{\mathbf{y}}_{aux}(\gamma) = -\mathbf{H}_{aux}\mathbf{H_y}^{-1}\gamma \tag{25}$$

Equations (24) and (25) will be used in the Results section to evaluate the biases' effects for a particular engine.

ESTIMATION OF THE EDPs WITH A LUENBERGER OBSERVER BASED ON THE SSVM

The linear approximation of the engine model given by equations (4) can only reproduce, with reasonable accuracy, quasi-stationary phenomena (i.e., small values of u's, x's, and y's as defined in eqs. (3) and eq. (5)). This circumstance has been taken into account in practice by the simple rule of deactivating the estimation process during engine transients (this rule is consistent with the objectives of the PSC algorithm, which only attempts to optimize the engine in steady state). Consequently, the data fed into the estimation process are acquired mostly during steady state. This opens up the question whether a dynamic model, different from the (steady-state) optimization model, is justified in practice for the PSC algorithm's estimation process. As an alternative, we next consider an η-estimator based on the engine's SSVM.

Starting from equation (11), we rewrite the measurable input/output relationship of the SSVM as follows:

$$\dot{\eta} = 0 \tag{26a}$$

$$\mathbf{y} = \mathbf{G}_y \mathbf{u} + \mathbf{H}_y \eta \tag{26b}$$

Following the same ideas as those used to prove Proposition 1 in Appendix A, it can be shown that, since $\mathbf{H}_y$ is nonsingular, the model equations (26) is observable. Consequently, a Luenberger observer (ref. 9) can be used to estimate the vector η.

The steady-state model-based Luenberger observer (SSMLO) equations are:

$$\dot{\hat{\eta}} = -\mathbf{K}(\hat{\mathbf{y}} - \mathbf{y}) \tag{27a}$$

$$\hat{\mathbf{y}} = \mathbf{G}_y \mathbf{u} + \mathbf{H}_y \hat{\eta} \tag{27b}$$

If one defines: $\tilde{\eta} \overset{\triangle}{=} \hat{\eta} - \eta$, from equations (26a, b) and equations (27a, b) one has:

$$\dot{\tilde{\eta}} = -\mathbf{K}(\hat{\mathbf{y}} - \mathbf{y}) = -\mathbf{K}\mathbf{H}_y \tilde{\eta} \tag{27c}$$

Now, since $\mathbf{H}_y$ is nonsingular, one can always find $\mathbf{K} \in \mathbb{R}^{5 \times 5}$ such that $\mathbf{K}\mathbf{H}_y$ has any desired eigenvalues. In particular, $\mathbf{K}$ is chosen to give:

$$\mathbf{K}\mathbf{H}_y = \Lambda = \begin{bmatrix} \lambda_1 & 0 & \dots & 0 \\ 0 & \lambda_2 & \dots & 0 \\ \vdots & \vdots & \ddots & 0 \\ 0 & 0 & 0 & \lambda_5 \end{bmatrix} \Rightarrow \mathbf{K} = \Lambda \mathbf{H}_y^{-1} \tag{28}$$

with $\lambda_1, \lambda_2, \dots, \lambda_5$, used as tuning parameters, any set of five negative real constants. The selection of the λ_i's is the result of a compromise between speed and noise rejection. As opposed to the KF, the tuning parameters are directly the (inverse of the) time constants of each of the estimated variables, which can thus be independently adjusted.

With equation (28), $\mathbf{K}$ can be calculated online with the current $\mathbf{H}_y$ that (together with $\mathbf{G}_y$ in eq. (27b)) is available at any time for the optimization model. An independent model for the estimation process is, thus, no longer needed. Moreover, the approximation consisting of using an estimation model different from the optimization model is eliminated. To summarize, the advantages of this method with respect to the estimator given by equations (6) to (9), concern the implementation, design, and tuning and are:

1. Contrary to the KF approach, the SSMLO does not require the storage and in-flight selection of the matrices $\mathbf{A}$, $\mathbf{B}$, $\mathbf{C}$, $\mathbf{D}$, $\mathbf{L}$, $\mathbf{M}$, and $\mathbf{K}$. The model used for estimation is the same as the model used for optimization.

2. The dimension and complexity of the estimator's equations have been reduced.

3. All the eigenvalues of the estimator can be directly assigned resulting in a more straightforward designing and tuning than with the KF. By this means, for instance, the convergence speed can easily be made independent of the power setting.

It must be noticed though that the proposed SSMLO estimator does not avoid the biases' effects. Actually those effects are a consequence of an intrinsic structural property of the system such as its observability (or *unobservability* in this case) and, hence, independent of the kind of η-estimator used.

If the measurements $\mathbf{u}$ and $\mathbf{y}$ are assumed to be corrupted by additive, stationary, and centered noises, respectively: ω and ρ, with corresponding covariance matrices: $\mathbf{Q} = E\{\omega\omega^T\}, \mathbf{R} = E\{\rho\rho^T\}$, the covariance of the estimation error:

$$\mathbf{P}(t) \stackrel{\triangle}{=} E\{\tilde{\eta}(t)\tilde{\eta}(t)^T\}$$

can be calculated using a standard result in the theory of stochastic linear systems (see for instance ref. 8, p. 70). For the case of the SSMLO estimator, equations (27), it can be shown that:

$$\dot{\mathbf{P}}(t) = -\Lambda\mathbf{P}(t) - \mathbf{P}(t)\Lambda + \Lambda\mathbf{H}_y^{-1}\left(\mathbf{R} + \mathbf{G}_y\mathbf{Q}\mathbf{G}_y^T\right)\left(\mathbf{H}_y^{-1}\right)^T\Lambda$$

Since Λ is, by assumption, a stable matrix, an *a priori* evaluation of the asymptotic covariance matrix $\mathbf{P}$ can be obtained by equating to zero the right-hand side of the last expression. For instance, if the estimator design is such that: $\Lambda = \lambda I$, one easily shows that:

$$\mathbf{P}(\infty) \stackrel{\triangle}{=} \frac{\lim \mathbf{P}(t)}{t \to \infty} = \frac{1}{2}\lambda\mathbf{H}_y^{-1}\left(\mathbf{R} + \mathbf{G}_y\mathbf{Q}\mathbf{G}_y^T\right)\left(\mathbf{H}_y^{-1}\right)^T$$

RESULTS

Quantitative Study of the Biases' Effects

Here we use the results of the Observability Conditions and Equivalence Between Biases and EDPs section to measure the influence of the biases on the estimation errors of the auxiliary variables. This allows us to determine (1) which measurement biases are more influential and, thus, where to

concentrate the efforts to improve the instrumentation, and conversely, (2) which of the estimated propulsion variables are affected the most by the presence of the biases.

All the variables, including the EDPs, are normalized to allow the comparison of magnitudes of different physical nature under a single scale. For the EDPs the normalizing factors are chosen as the maximum expected engine deviations with respect to a nominal engine. For the rest of the variables, the normalizing factors were selected according to what experience shows as a "reasonable" typical range excursion for each variable during PSC flight testing. The chosen normalizing values are stated in Appendix C. The normalized variables give us the possibility to discern between the qualitative notions of "big" and "small" perturbations. For instance, a "big" perturbation or a "big" bias is one that is "somewhat" comparable with a "typical" excursion in the corresponding variable.

The study is carried out over the whole range of $PT4$ of the reference flight conditions without afterburner. Given the close relationship between $PT4$ and the engine's power, the results illustrate the influence of the power setting on the accuracy of the estimation.

Effects of the input biases We now use equation (24) to study the effects of the input biases over the estimation errors of the auxiliary variables for each local model indexed by $PT4$. All the magnitudes are expressed in percentages of the normalizing factors (given in Appendix B). The effects are plotted in figures 3 to 6 (one figure for each input) as a function of $PT4$.

A comparison between the figures shows that the influence of the biases in WF is orders of magnitude bigger than that of the rest of the inputs (notice in particular the important effects on $WCHPC$). From the enlargement of figure 3(a) given in figure 3(b), one sees that $TT6$ and $WCFAN$ are also considerably affected. Figures 3 through 6 show that the biases in $CIVV$ and $RCVV$ don't have a significant incidence on the estimates. The effects of biases in AJ are mainly perceived in the estimation of $WCFAN$. Notice that, unlike the effects of the bias in WF, the influence of a bias in AJ increases with the power level.

In terms of the possible biases affecting the inputs, we thus conclude that: (1) WF is largely the most critical input variable and its effects are particularly strong for low power settings; (2) the biases in $CIVV$ and $RCVV$ do not have any significant influence on the estimated variables; (3) biases in AJ have a significant influence on the estimation of $WCFAN$; (4) only the estimates of $WCHPC$, $WCFAN$, and $TT6$ are considered to be affected by the input biases.

Effects of the output biases Similarly as before, but now using equation (25), figures 7 to 11 show plots of the normalized estimation errors of the auxiliary variables induced by a 1-percent bias on the output measurements (one figure for each output). The effects of the output biases are comparable to those caused by the input biases (except for WF). A 1-percent bias in $FTIT$, $PT6$, and $N1$ produces estimation errors greater than 2 percent in the middle- and high-power ranges. A bias in $N2$ has influence only at higher power settings and concerns, mainly, $TT3$ and $TT4$. The biggest errors are produced by biases in $FTIT$ and affect $WCHPC$ (4 to 6 percent errors).

In terms of possible biases affecting the output, we thus conclude that: (1) biases in $FTIT$, $PT6$, $N1$, and $N2$ (in that order) have a noticeable effect on the estimations; though, given the generally good quality of the measurements of $N1$ and $N2$ one may be concerned only by $FTIT$ and $PT6$; (2)

14

as with the input biases, the estimations most affected are $WCHPC$ and $WCFAN$ (see figs. 7, 10, and 11). To a lesser extent, $TT6$, $TT4$, and $TT3$ are also affected.

Evaluation of the SSMLO Approach

We now review the estimation approach proposed in the Estimation of the EDPs with a Luenberger Observer and the SSVM section. For this review, a comparison with the KF approach is performed using real flight data. As shown before, the SSMLO approach is not supposed to alter the influence of the biases, thus no conclusion concerns this aspect.

Flight conditions The data were collected during a cruise steady-state flight test condition at 30,000-ft altitude, Mach 0.91, and 60° power lever angle, with the PSC algorithm in the minimum fuel mode. All the variables are normalized using the normalization factors given in Appendix B, and referred to the local base point:

$$[N1\ N2\ PT4\ FTIT\ PT6]_b = \left[8661\ \text{rpm},\ 11,844\ \text{rpm},\ 160\ \text{lb/in}^2,\ 1854\ °\text{F},\ 19.29\ \text{lb/in}^2\right];$$

$$[WF\ AJ\ CIVV\ RCVV\ HPX\ BLD]_b = \left[4150\ \text{lb/hr},\ 435.23\ \text{in}^2,\ -2.59°,\ 2.27°,\ 0\ \text{hp},\ 0\ \text{lb/in}^2\right]$$

Figures 12(a) and 12(b) are plots of the normalized deviations with respect to the base point of the measured inputs and outputs, respectively, sampled at 8 Hz.

Results With equation (28) we have the choice of arbitrarily selecting the observer's dynamics. An observer's settling time of 20 sec was considered adequate for the application. Accordingly, the following set of eigenvalues was selected:

$$\lambda_1 = -0.3; \lambda_2 = -0.2; \lambda_3 = -0.3; \lambda_4 = -0.3; \lambda_5 = -0.3 \tag{29}$$

An originally $\lambda_2 = -0.3$ value was modified *a posteriori* in order to improve the noise rejection capability of the estimator.

In figures 13(a) and 13(b), the EDPs estimated using the KF are compared with those obtained with the SSMLO using the same data. The initial EDPs' estimated values are assumed zeros for both estimators. As expected, both estimators converge to the same asymptotic values. The settling times of the SSMLO's estimates are in plain correspondence with the specified λ_i's (four to five times the corresponding time constants: $1/\lambda_i$). For the KF, the settling times range from 6 to 8 sec for $DEHPT$ or $AAHT$, to approximately 35 sec for $DELPT$. Note that there is a high-frequency residual noise with the KF. This is a consequence of its larger bandwidth associated with its fast modes (see also item (4) in the listing within the Estimation of the EDPs With a Luenberger Observer and the SSVM section).

The auxiliary variables are estimated with both algorithms. In each case, the value of η is substituted in equation (10) by the corresponding estimate. The results for the KF and those for the SSMLO are compared in figure 14. Notice how the choice of eigenvalues (eq. (29)) reduces the long time constant associated with the KF's estimation of $DELPT$. As seen in figure 14, this translates into faster estimates of $WCFAN$ and $WCHPC$.

CONCLUDING REMARKS

The engine deviation parameter estimates do not necessarily quantify the engine's off-nominal behavior. For instance, it is impossible to distinguish the effects produced on the estimates by an off-nominal engine condition from those caused by measurement biases. Actually, the off-nominal behavior can be equivalently characterized by additive terms (biases) on the measured input and output data. For performance seeking control application, a given engine off-nominal characterization needs to be evaluated through the effects that model inaccuracies (e.g., the biases) may have on the predictions provided by the optimization model. The accuracy with which the latter predicts the output variables is the ultimate measure of the effectiveness of the estimation process. Here, the errors induced by the biases on the calculated auxiliary variables are used as a measure of the effectiveness of the estimation process and the measurement system. It is thus determined that the most critical measurements are gas generator fuel flow (WF), nozzle throat area (AJ), fan turbine inlet temperature ($FTIT$), and afterburner inlet total pressure ($PT6$). Unknown biases on those measurements may have a strong effect on the optimization through a wrong forecast of the engine's variables. Among the latter measurements, the most affected are corrected high-pressure compressor airflow ($WCHPC$), corrected fan airflow ($WCFAN$), and afterburner inlet total temperature ($TT6$).

With the Kalman filter approach, two independent sets of local linear models need to be stored in memory. With the new proposed technique the estimation and optimization processes share the same piecewise linear model. Thus, no extra online model switching is required, less computer memory is needed, and the identity between the local optimization model and the local estimation model is guaranteed at all moments. Furthermore, the filter's dynamics can be made independent of the power setting. The tests with flight data show that the neglected engine's dynamics do not have any noticeable effects on the estimates, and that similar or better noise rejection and convergence speed can be obtained with the new scheme.

The open-loop nature of the performance seeking control scheme makes it very sensitive to model–engine mismatches and in particular to measurement biases. We show that an apparent estimated engine deviation may only be the effect of unknown biases. Under these conditions trying to improve the peformance of an engine in apparent "good shape" (that in fact isn't) could lead toward the violations of the safety limits. Conversely if the engine is better than it seems through the estimation process, a too conservative control will not take advantage of the engine's actual capabilities. Consequently it is conceivable in this case that the performance seeking control system will issue commands leading to a worse performance than the one obtained with the nominal model in the nonadaptive case. This conclusion strongly demonstrates the need for developing new adaptive performance optimization techniques less sensitive to an *a priori* engine model and based on the feedback of the actual performance measure.

APPENDIX A

PIECEWISE LINEARIZATION: THE GENERAL PRINCIPLE

We first describe the general principle of the multimodel linear approximation of a general dynamic nonlinear system. Let:

$$\dot{x} = f(x, u) \tag{A-1a}$$

$$y = h(x, u) \tag{A-1b}$$

with f and h differentiable with respect to their respective arguments be the mathematical model of a (nonlinear) system where: $x \in \mathbb{R}^n$ is the state vector, $y \in \mathbb{R}^m$ is the measurable output vector, and $u \in \mathbb{R}^p$ is the input vector. The equilibria of system (A-1) are given by the equations:

$$f(x^o, u^o) = 0 \tag{A-2a}$$

$$y^o = h(x^o, u^o) \tag{A-2b}$$

Since the independent variable u^o ranges within a continuum of values, the solutions (x^o, y^o, u^o) of (A-2) will also be a continuum subset of $\mathbb{R}^n \times \mathbb{R}^m \times \mathbb{R}^p$, we call this set $E \subset \mathbb{R} \times \mathbb{R}^m \times \mathbb{R}^p$. Now, given a point $p = (x^o, y^o, u^o) \in E$, let us define:

$$\delta x: = x - x^o; \quad \delta u: = u - u^o; \quad \delta y: = y - y^o \tag{A-3}$$

Given that $f(x^o, u^o) = 0$, the linear part of:

$$\delta \dot{x} = f_x(x^o, u^o)\delta x + f_u(x^o, u^o)\delta u$$
$$+ o(\| \delta x \|^2, \| \delta u \|^2) \tag{A-4a}$$

$$\delta y = h_x(x^o, u^o)\delta x + h_u(x^o, u^o)\delta u$$
$$+ o(\| \delta x \|^2, \| \delta u \|^2) \tag{A-4b}$$

(i.e.; the linearization of (A-1) around p) represents a "good" approximation of (A-1) within a "sufficiently small ball $V(p)$" around the point $p = (x^o, y^o, u^o)$. Let us define $L \subset \mathbb{R}^n \times \mathbb{R}^m \times \mathbb{R}^p$ as:

$$L = \bigcup_{p \in E} V(p) \tag{A-5}$$

L is the region within which (A-1) can be approximated by the collection of linear models represented by (A-4). Within this "linearity region," however, only quasi-stationary phenomena can take place. In fact, the higher order terms in (A-4) can only be neglected for x and u sufficiently near the equilibrium condition given by (A-2a).

Now, if given u^o there are unique $x^o(u^o)$ and $y^o(Au^o)$ satisfying (A-2), the quasi-stationary solutions of (A-1) can be approximated by the solutions of the following equations:

$$\delta \dot{x} = A(u^o)\delta x + B(u^o)\delta u \tag{A-6a}$$

$$\delta y = C(u^o)\delta x + D(u^o)\delta u \tag{A-6b}$$

Where

$$\delta u: = u - u^o; \quad \delta x: = x - x^o(u^o); \quad \delta y: = y - y^o(u^o)$$

and

$$A(u^o) = f_x(x^o, u^o); \quad B(u^o) = f_u(x^o, u^o) \tag{A-7a}$$

$$C(u^o) = h_x(x^o, u^o); \quad D(u^o) = h_u(x^o, u^o) \tag{A-7b}$$

The local linear model (its origin and dynamic equations) is thus completely determined by the value of u^o. After discretizing the admissible set of values of u^o, (A-6) may be used to create a table relating the discrete values of u^o with the corresponding linear models. To determine a valid local model, an algorithm must still be provided to decide when the present local model is no longer valid, and to choose a new model from the tables (possibly by interpolation).

Parameterizing the Model–System Mismatch

In practice, the mathematical model (A-1) may not represent the real system with sufficient accuracy. Among the reasons for this situation are: one counts not only the typical approximations and modeling inaccuracies, but also changes in the system itself resulting from aging, deterioration, off-nominal operation, etc. Under these conditions, a distinction should be made between the model (A-1) and the "true" system's equations that we denote by:

$$\dot{x} = f^s(x, u)$$

$$y = h^s(x, u)$$

In general, $f \neq f^s$ and $h \neq h^s$ thus for (x^o, u^o) a given steady-state solution of (A-1) $f^s(x^o, u^o) \neq 0$, and one has:

$$\dot{x} = \delta\dot{x} = f^s(x, u) = f^s(x^o, u^o) + f_x^s(x^o, u^o)\delta x + f_u^s(x^o, u^o)\delta u$$

$$+\text{``higher order terms''} \tag{A-8a}$$

$$\delta y = y - y^o = h^s(x^o, u^o) - h(x^o, u^o) + h_u^s(x^o, u^o)\delta x + h_u^s(x^o, u^o)\delta u$$

$$+\text{``higher order terms''} \tag{A-8b}$$

Notice that the model–system mismatch introduces additive constant terms in the dynamic as well as in the output equations (biases) and modifies the local linear dynamics (compare eqs. (A-8) with eqs. (A-4) and (A-5)). A strong assumption consists in saying that the mismatch can be characterized by a vector $\eta \in \mathbb{R}^q$ with components called deviation parameters. Under this supposition, the "real system" is represented (similarly as in eq. (A-1)) by:

$$\dot{x} = f^s(x, u) = f(x, u, \eta) \tag{A-9a}$$

$$y = h^s(x, u) = h(x, u, \eta) \tag{A-9b}$$

while the "nominal system" corresponds to the value of $\eta = 0$. As before, the base points are determined by the nominal system's equations and satisfy $f(x^o, u^o, 0) = 0$. Thus, with equations (A-8) and (A-9), and assuming small deviations, one can write the following expansion:

18

$$\delta\dot{\mathbf{x}} = (\mathbf{f_x}(\mathbf{x}^o,\ \mathbf{u}^o,\ 0) + \mathbf{f_{x\eta}}(\mathbf{x}^o,\ \mathbf{u}^o,\ 0) \otimes \eta)\delta\mathbf{x} + (\mathbf{f_u}(\mathbf{x}^o,\ \mathbf{u}^o,\ 0) + \mathbf{f_{u\eta}}(\mathbf{x}^o,\ \mathbf{u}^o,\ 0) \otimes \eta)\delta\mathbf{u}$$
$$+ \mathbf{f_\eta}(\mathbf{x}^o,\ \mathbf{u}^o,\ 0)\eta + \text{``}higher\ order\ terms\text{''} \tag{A-10a}$$

$$\delta\mathbf{y} = (\mathbf{h_x}(\mathbf{x}^o,\ \mathbf{u}^o,\ 0) + \mathbf{h_{x\eta}}(\mathbf{x}^o,\ \mathbf{u}^o,\ 0) \otimes \eta)\delta\mathbf{x} + (\mathbf{h_u}(\mathbf{x}^o,\ \mathbf{u}^o,\ 0) + \mathbf{h_{u\eta}}(\mathbf{x}^o,\ \mathbf{u}^o,\ 0) \otimes \eta)\delta\mathbf{u}$$
$$+ \mathbf{h_\eta}(\mathbf{x}^o,\ \mathbf{u}^o,\ 0)\eta + \text{``}higher\ order\ terms\text{''} \tag{A-10b}$$

where the symbol $\otimes$ is a short notation for the actual linear combination of matrices that should be performed in the above formulae (notice that $\mathbf{h}_{x\eta}$ and $\mathbf{h}_{u\eta}$ are three-dimensional matrices). Equations (A-10a and b) are similar to (A-8) and show, up to a first-order approximation, the incidence of η on the local linear model. Both the local dynamics and the corresponding steady-state operation point are affected by the deviations with respect to the nominal system. Only in the case when the product $\otimes$ can be neglected, expression (A-10) simplifies into:

$$\delta\dot{\mathbf{x}} = \mathbf{A}(\mathbf{u}^o)\delta\mathbf{x} + \mathbf{B}(\mathbf{u}^o)\delta\mathbf{u} + \mathbf{L}(\mathbf{u}^o)\eta + \text{``}higher\ order\ terms\text{''} \tag{A-11a}$$

$$\delta\mathbf{y} = \mathbf{C}(\mathbf{u}^o)\delta\mathbf{x} + \mathbf{D}(\mathbf{u}^o)\delta\mathbf{u} + \mathbf{M}(\mathbf{u}^o)\eta + \text{``}higher\ order\ terms\text{''} \tag{A-11b}$$

Where now,

$$\mathbf{A}(\mathbf{u}^o):\ = \mathbf{f_x}(\mathbf{x}^o,\ \mathbf{u}^o, 0);$$
$$\mathbf{B}(\mathbf{u}^o):\ = \mathbf{f_u}(\mathbf{x}^o,\ \mathbf{u}^o, 0);$$
$$\mathbf{L}(\mathbf{u}^o):\ = \mathbf{f_\eta}(\mathbf{x}^o,\ \mathbf{u}^o, 0);$$
$$\mathbf{C}(\mathbf{u}^o):\ = \mathbf{h_x}(\mathbf{x}^o,\ \mathbf{u}^o, 0);$$
$$\mathbf{D}(\mathbf{u}^o):\ = \mathbf{h_u}(\mathbf{x}^o,\ \mathbf{u}^o, 0);$$
$$\mathbf{M}(\mathbf{u}^o):\ = \mathbf{h_\eta}(\mathbf{x}^o,\ \mathbf{u}^o, 0); \tag{A-12}$$

APPENDIX B

PROOF OF PROPOSITION 1

Using standard results of the observability theory of linear systems, it can be readily shown that the model equations (4)/(6) are completely observable, if and only if the matrix:

$$\mathbf{O} = \begin{bmatrix} \mathbf{C} & \mathbf{M} \\ \mathbf{CA} & \mathbf{CL} \\ \mathbf{CA}^2 & \mathbf{CAL} \\ \vdots & \vdots \\ \mathbf{CA}^{n+p-1} & \mathbf{CA}^{n+p-2}\mathbf{L} \end{bmatrix}$$

has rank $n + p$. But, since as it can be easily shown:

$$\mathbf{O} = \begin{bmatrix} \mathbf{I}_m & 0 \\ 0 & \mathbf{C} \\ 0 & \mathbf{CA} \\ \vdots & \vdots \end{bmatrix} \begin{bmatrix} \mathbf{C} & \mathbf{M} \\ \mathbf{A} & \mathbf{L} \end{bmatrix},$$

rank($\mathbf{O}$) = $n + p$ only if $\mathbf{S}$ in equation (12) is such that: rank($\mathbf{S}$) $\geq n + p$.

APPENDIX C

NORMALIZING FACTORS

Input variables normalizing factors	WF, lb/hr 2000.0	AJ, in^2 20.0	$CIVV$, deg 5.0	$RCVV$, deg 5.0
Output variables normalizing factors	$N1$, rpm 1000.0	$N2$, rpm 1000.0	$PT4$, lb/in^2 50.0	
	$FTIT$, °F 200.0	$PT6$, lb/in^2 5.0		
Auxiliary output variables normalizing factors	$TT6$, °F 200.0	$WCFAN$, lb/sec 20.0	$PT2.5$, lb/in^2 5.0	$TT2.5$, °F 50.0
	$TT3$, °F 100.0	$TT4$, °F 200.0	$WCHPC$, lb/sec 2.0	
EDP ranges	$DEHPT$, percent 1.0	$DELPT$, percent 1.0	$DWHPC$, lb/sec 60.0	
	$DWFAN$, lb/sec 255.0	$AAHT$, in^2 60.0		

REFERENCES

1. Luppold, R.H., G. Gallops, L. Kerr, and J.R. Roman, "Estimating In-Flight Engine Performance Variations Using Kalman Filter Concepts," AIAA-89-2584, July 1989.

2. Gilyard, Glenn B. and John S. Orme. "Subsonic Flight Test Evaluation of a Performance Seeking Control Algorithm on an F-15 Airplane," AIAA-92-3743, July 1992. Also printed as NASA TM-4400, 1992.

3. Nobbs, S.G., S.W. Jacobs, and D.J. Donahue, "Development of the Full-Envelope Performance Seeking Control Algorithm," AIAA-92-3748, July 1992.

4. Orme, John S. and Glenn B. Gilyard, "Subsonic Flight Test Evaluation of a Propulsion System Parameter Estimation Process for the F100 Engine," AIAA-92-3745, July 1992. Also printed as NASA TM-4426, 1992.

5. Orme, John S. and Glenn B. Gilyard, "Preliminary Supersonic Flight Test Evaluation of Performance Seeking Control," AIAA-93-1821, June 1993.

6. Alag, Gurbux S. and Glenn B. Gilyard, "A Proposed Kalman Filter Algorithm for Estimation of Unmeasured Output Variables for an F100 Turbofan Engine," AIAA-90-1920, July 1990. Also printed as NASA TM-4234, 1990.

7. Kalman, R.E. and R.S. Bucy, "New Results in Linear Filtering and Prediction Theory," *J. Basic Engineering Transactions of the ASME, Series D*, no. 3, Mar. 1961, pp. 95–108.

8. Kailath, T., *Lectures on Wiener and Kalman Filtering*, CISM Courses and Lectures no. 140, International Centre for Mechanical Sciences, Springer-Verglag Wien, New York, NY, 1981.

9. Wolovich, W.A., *Linear Multivariable Systems*, Applied Mathematical Sciences no. 11, Springer Verlag, New York, NY, 1974.

10. Åström, Karl Johan and Björn Wittenmark, *Computer Controlled Systems Theory and Design*, Prentice-Hall Information and System Sciences Series, Prentice-Hall Inc., Englewood Cliffs, NJ, 1984.

11. Åström, Karl Johan and Björn Wittenmark, *Adaptive Control*, Addison-Wesley Series in Electrical Engineering and Computer Engineering: Control Engineering, Addison-Wesley Publishing Co., Inc., New York, NY, 1989.
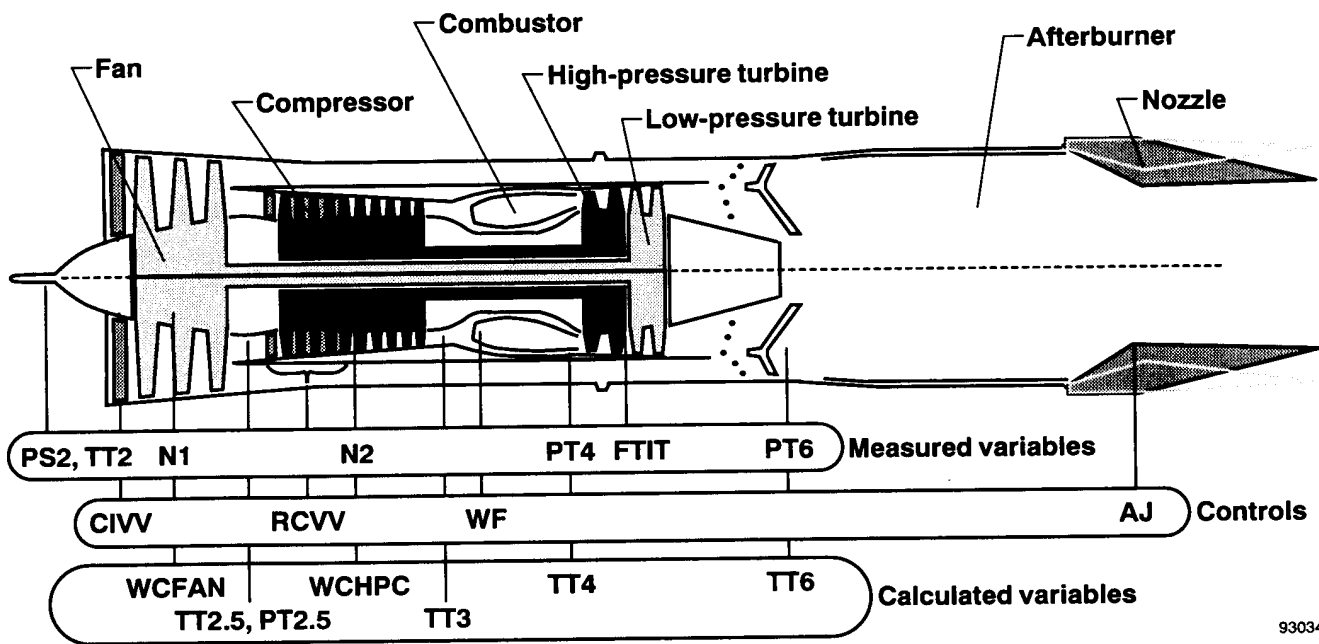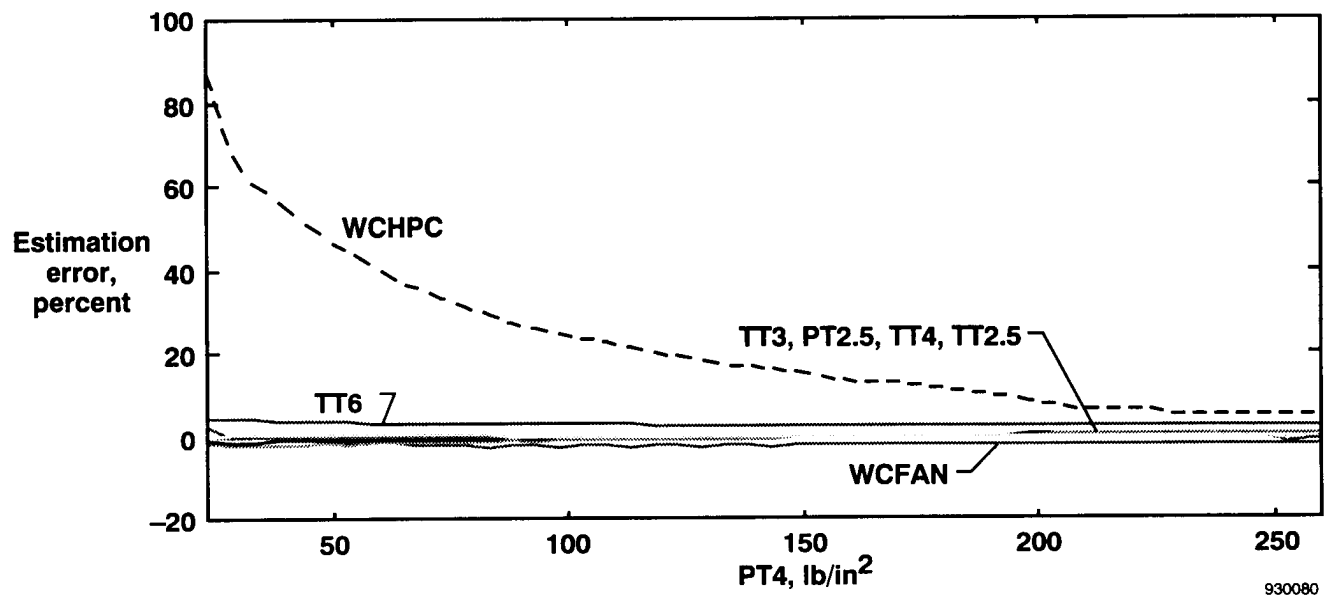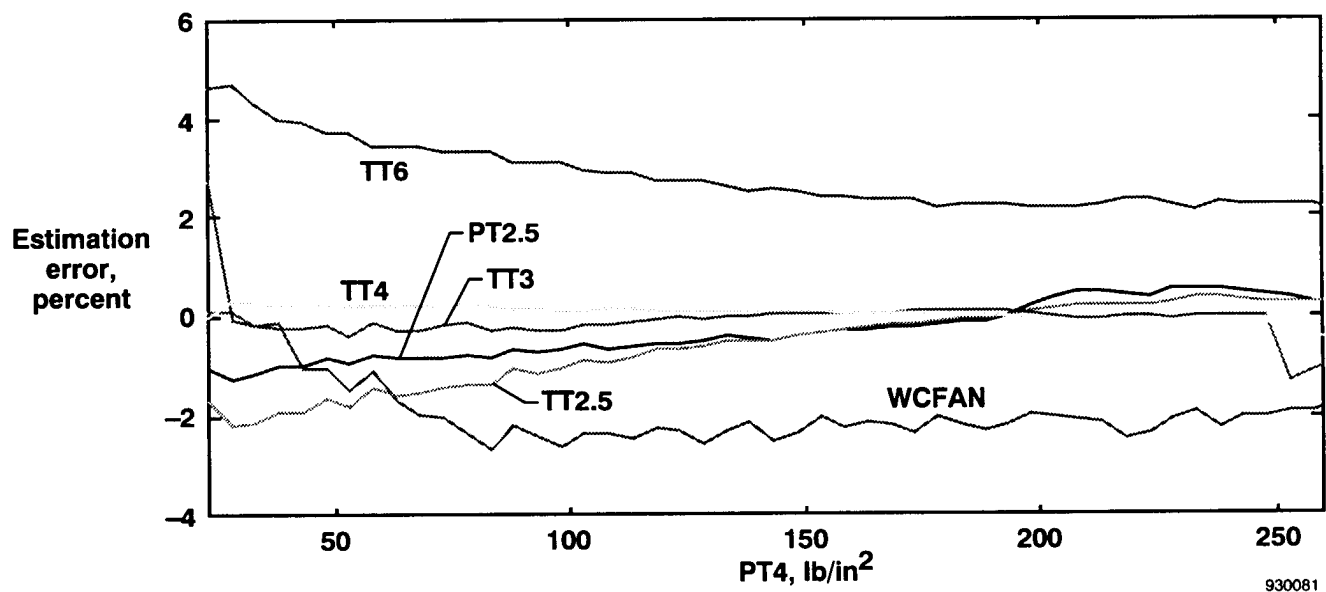
Fig. 1 F100 engine and locations of sensors.
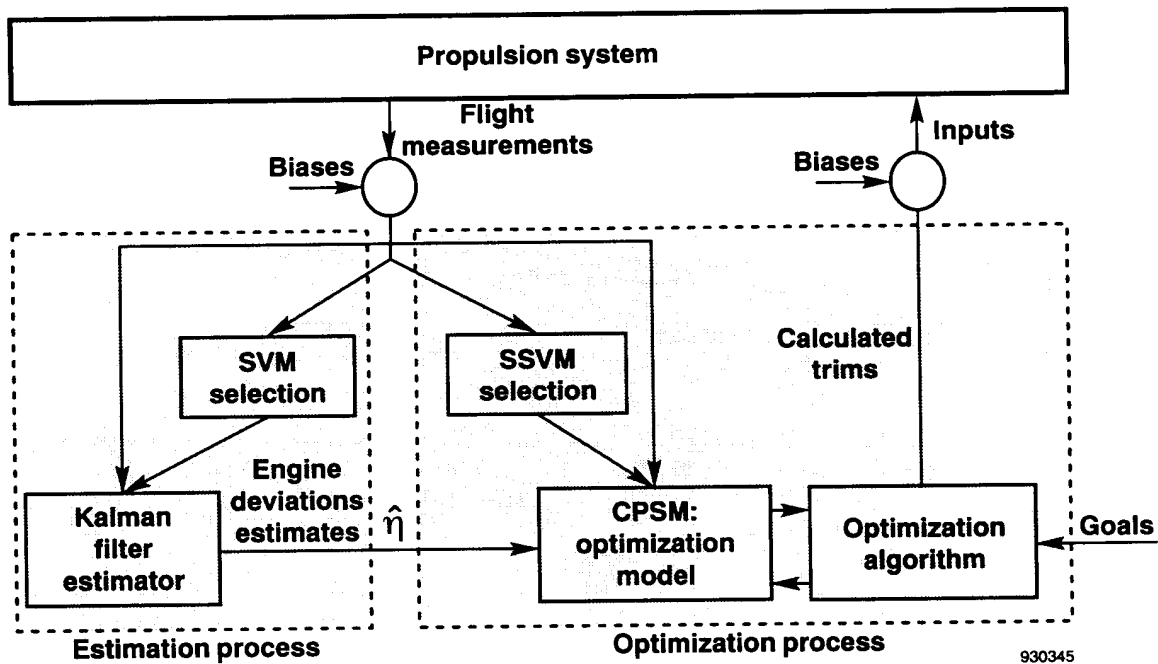
Fig. 2 Flow diagram of the PSC algorithm.

(a)

(b)

Fig. 3 Normalized auxiliary variable estimation errors resulting from a 1-percent bias in WF as a function of $PT4$.
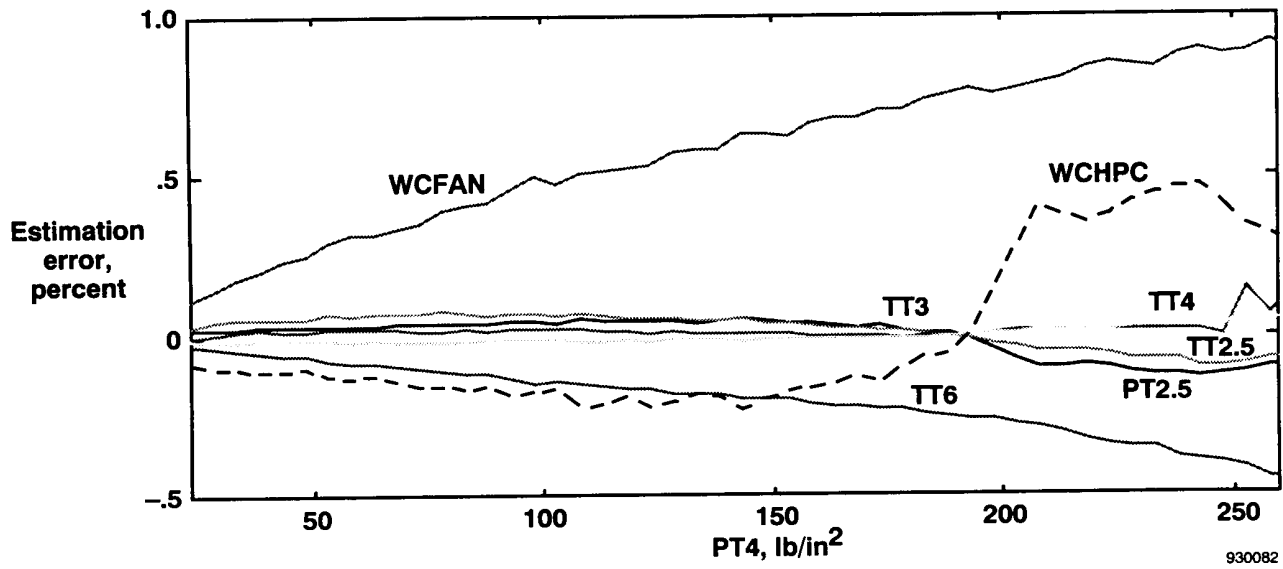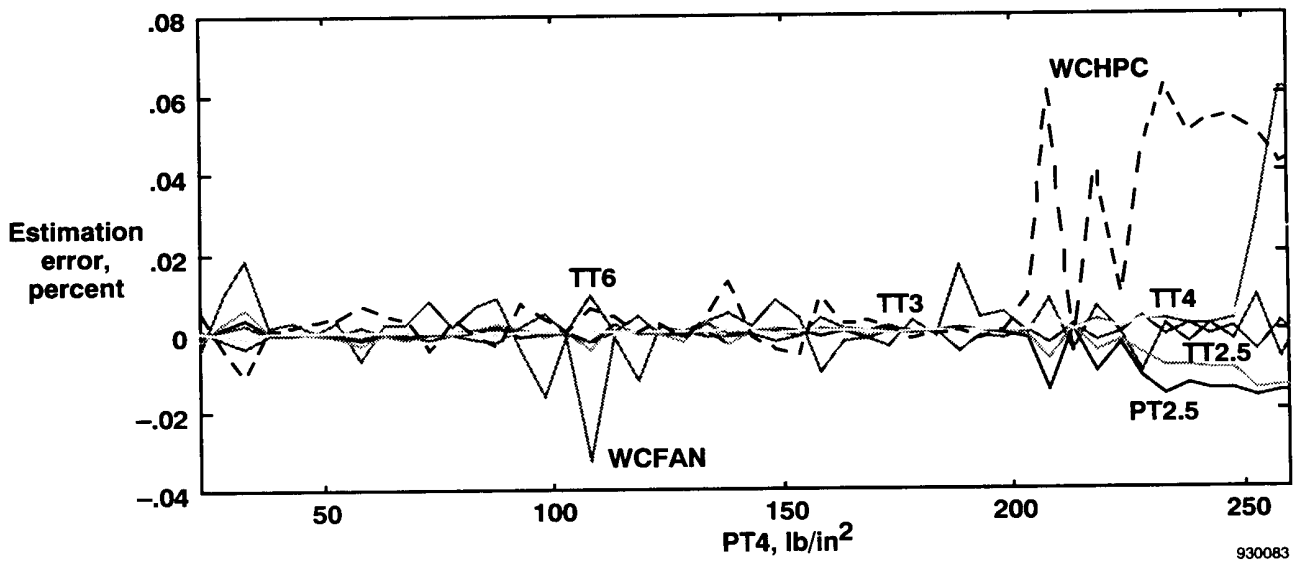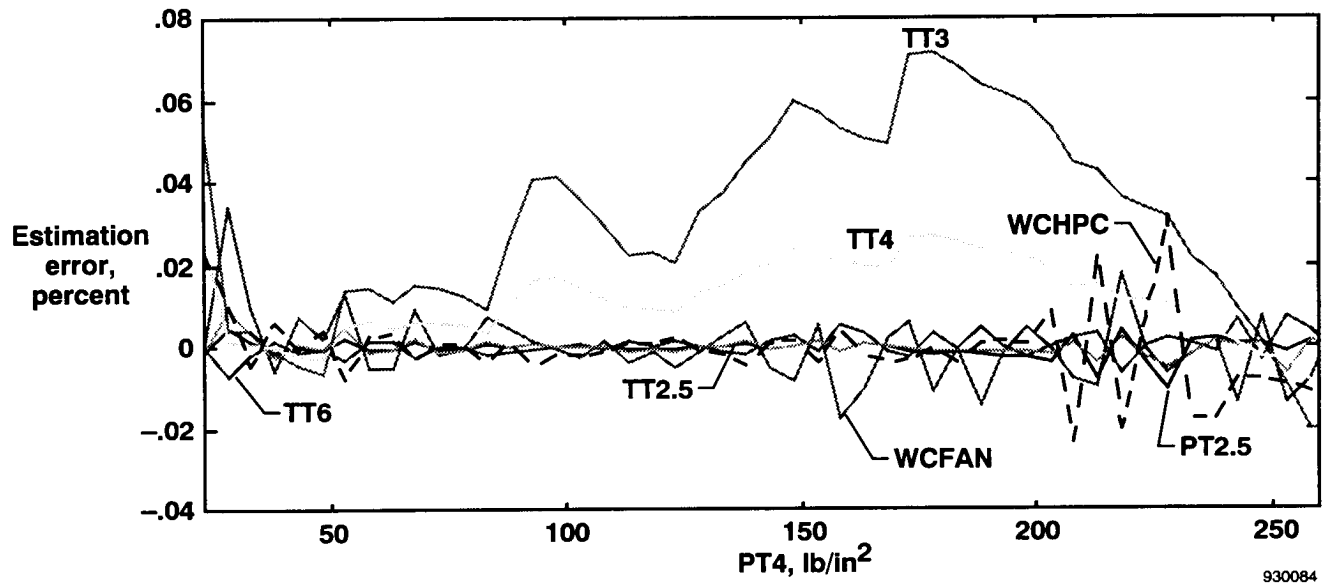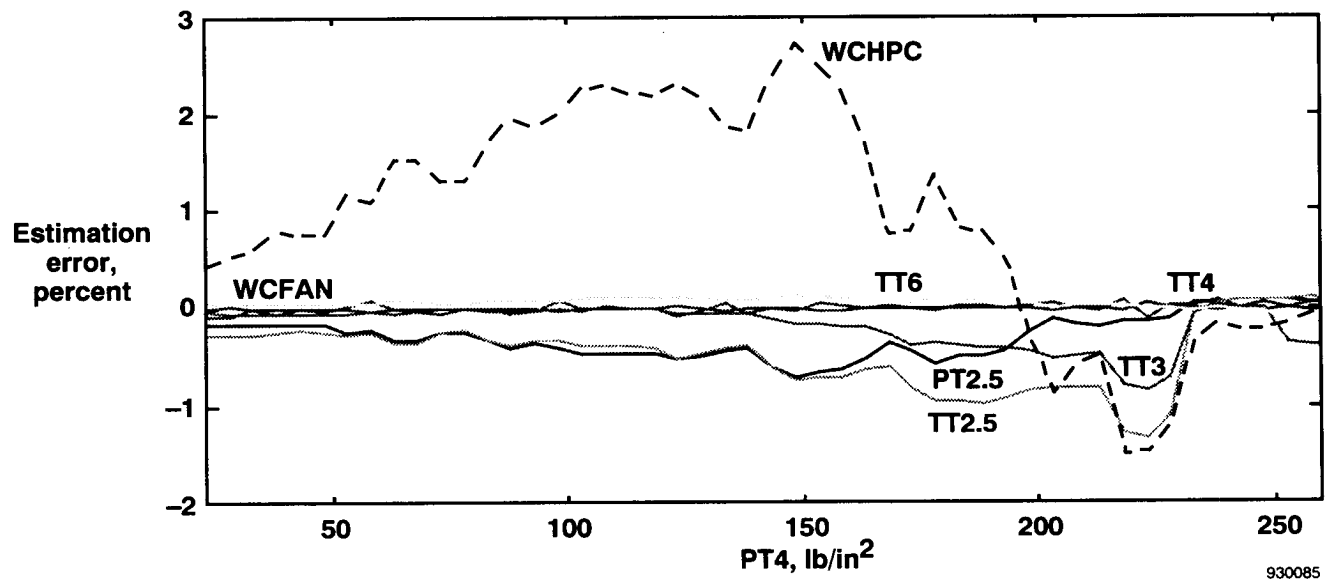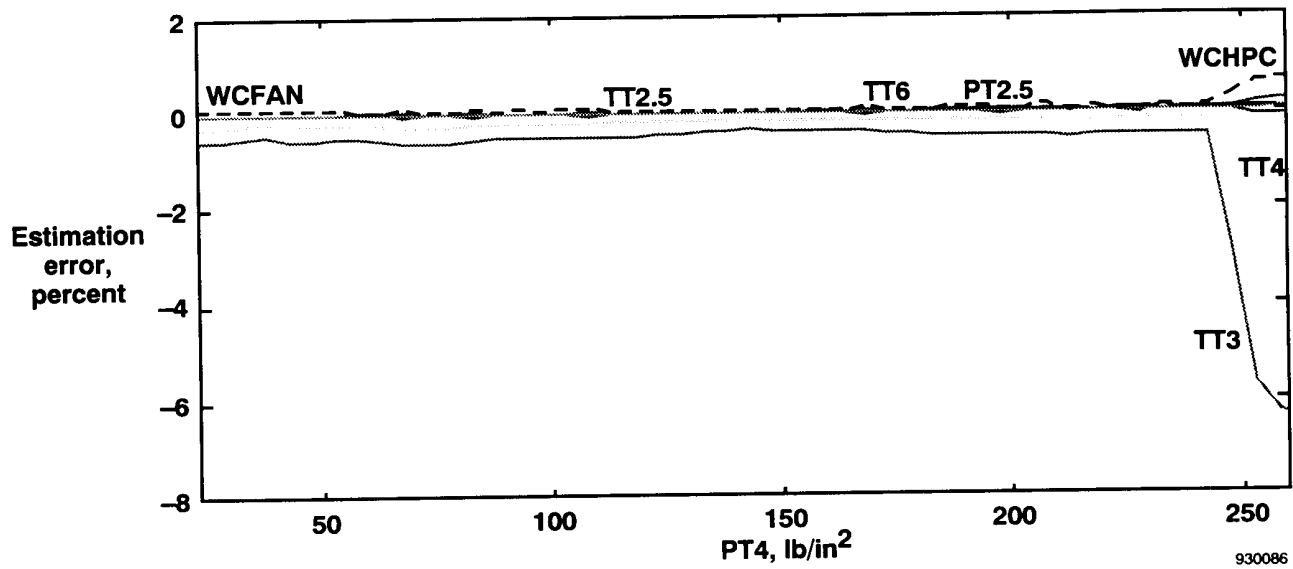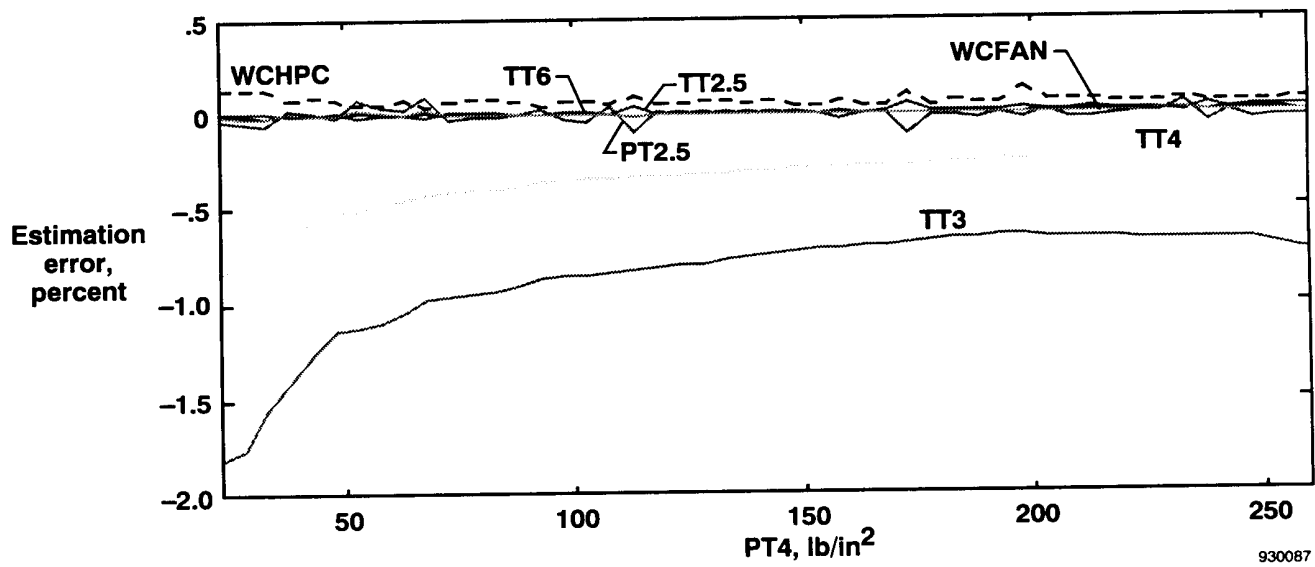
24

Fig. 4 Normalized auxiliary variable estimation errors resulting from a 1-percent bias in AJ as a function of $PT4$.
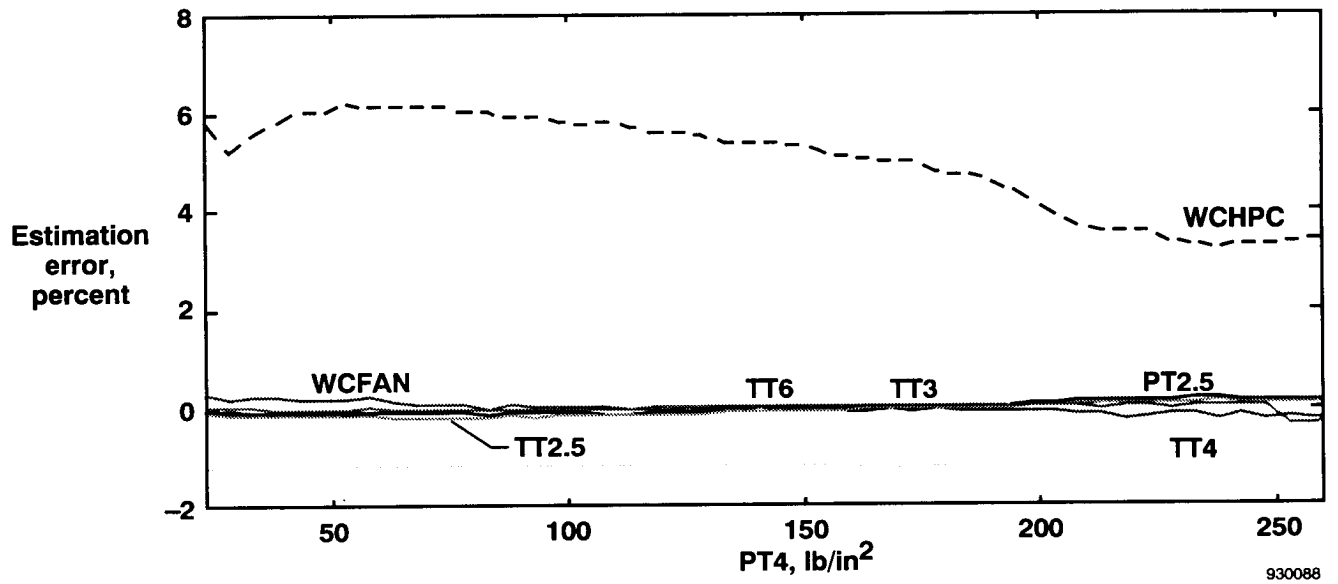

Fig. 5 Normalized auxiliary variable estimation errors resulting from a 1-percent bias in $CIVV$ as a function of $PT4$.

Fig. 6 Normalized auxiliary variable estimation errors resulting from a 1-percent bias in $RCVV$ as a function of $PT4$.
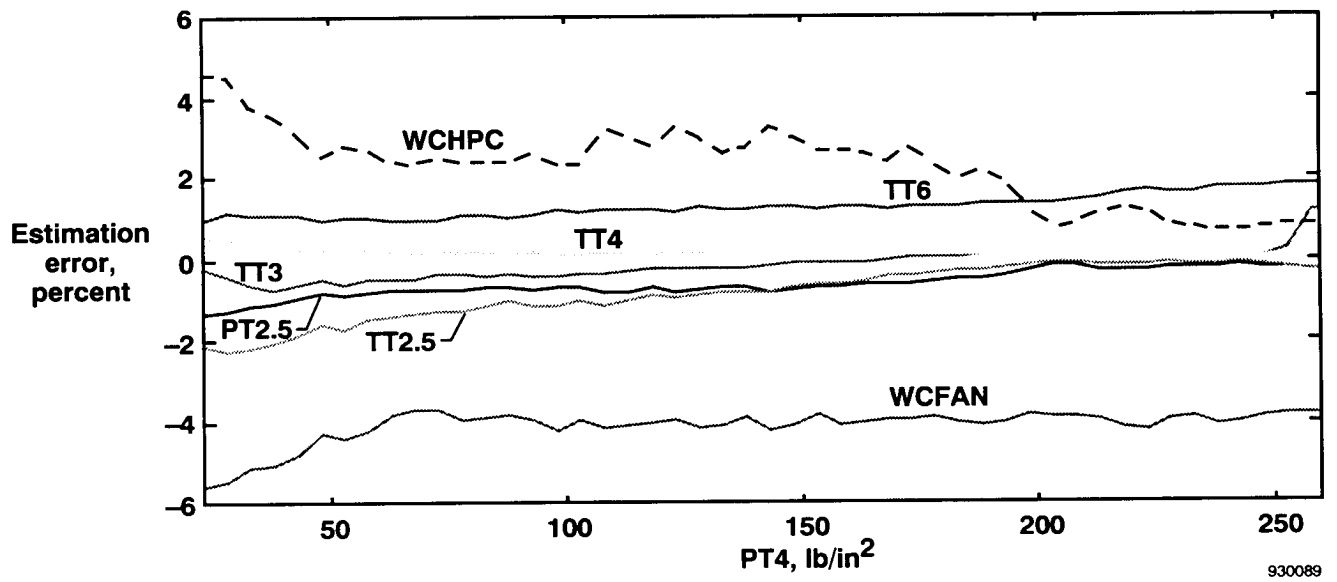

Fig. 7 Normalized auxiliary variable estimation errors resulting from a 1-percent bias in $N1$ as a function of $PT4$.

Fig. 8 Normalized auxiliary variable estimation errors resulting from a 1-percent bias in $N2$ as a function $PT4$.

Fig. 9 Normalized auxiliary variable estimation errors resulting from a 1-percent bias in $PT4$ as a function of $PT4$.

27

Fig. 10 Normalized auxiliary variable estimation errors resulting from a 1-percent bias in $FTIT$ as a function of $PT4$.
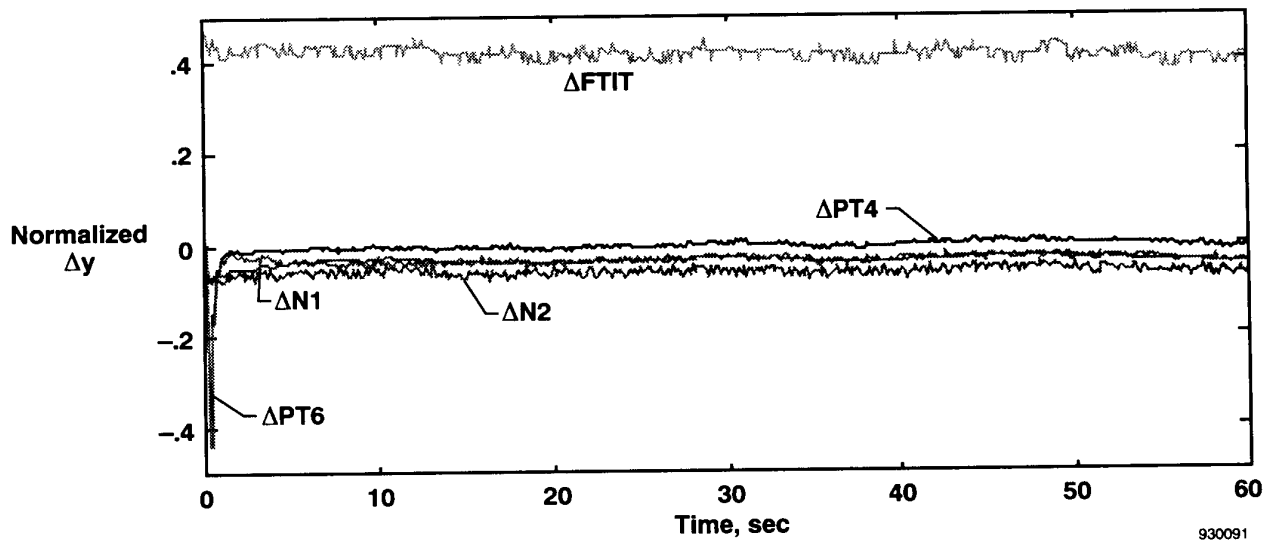

Fig. 11 Normalized auxiliary variable estimation errors resulting from a 1-percent bias in $PT6$ as a function of $PT4$.

28
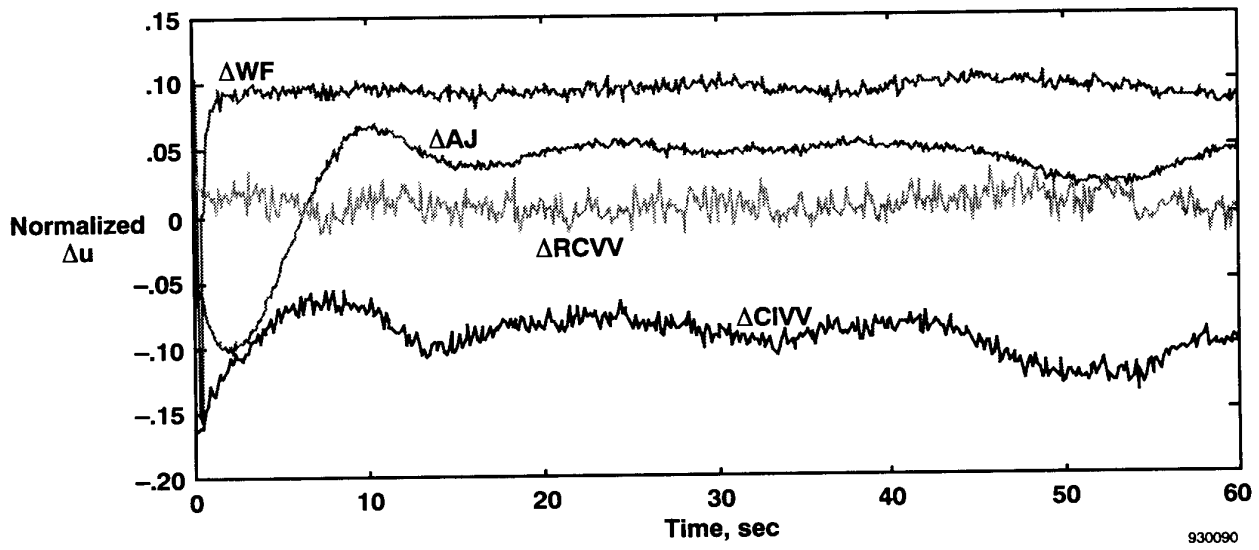
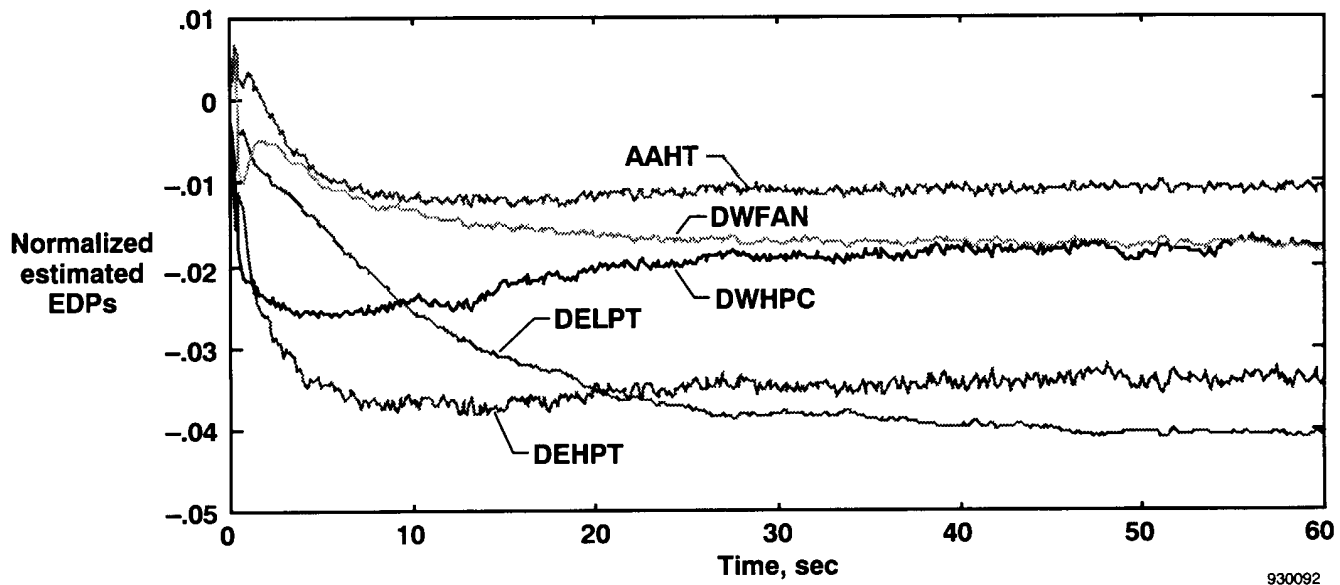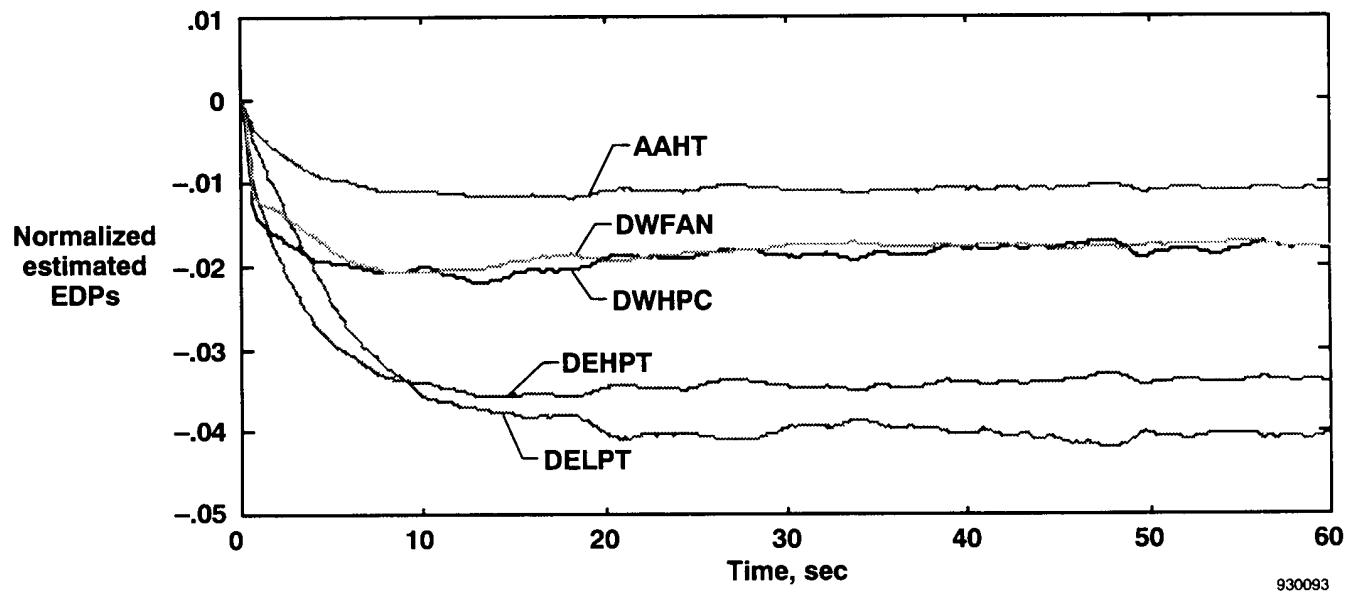(a) Input variables (Δu-vector).

(b) Output measured variables (Δy-vector).

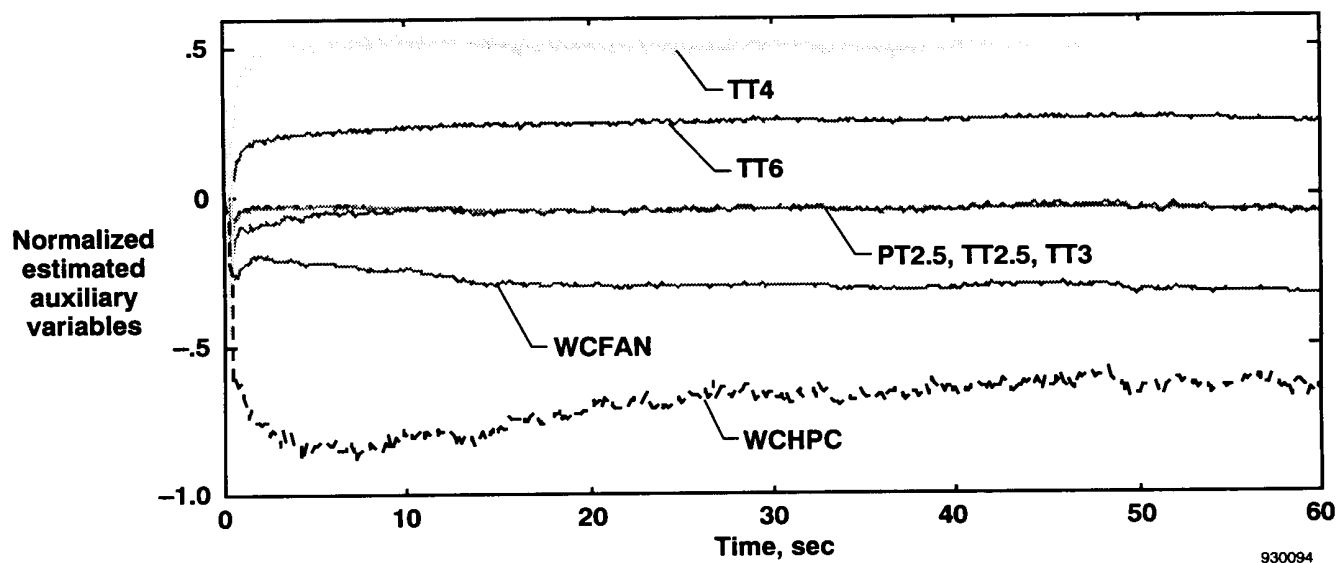Fig. 12 Normalized incremental variables sampled at 8 Hz.

29

(a) KF approach.

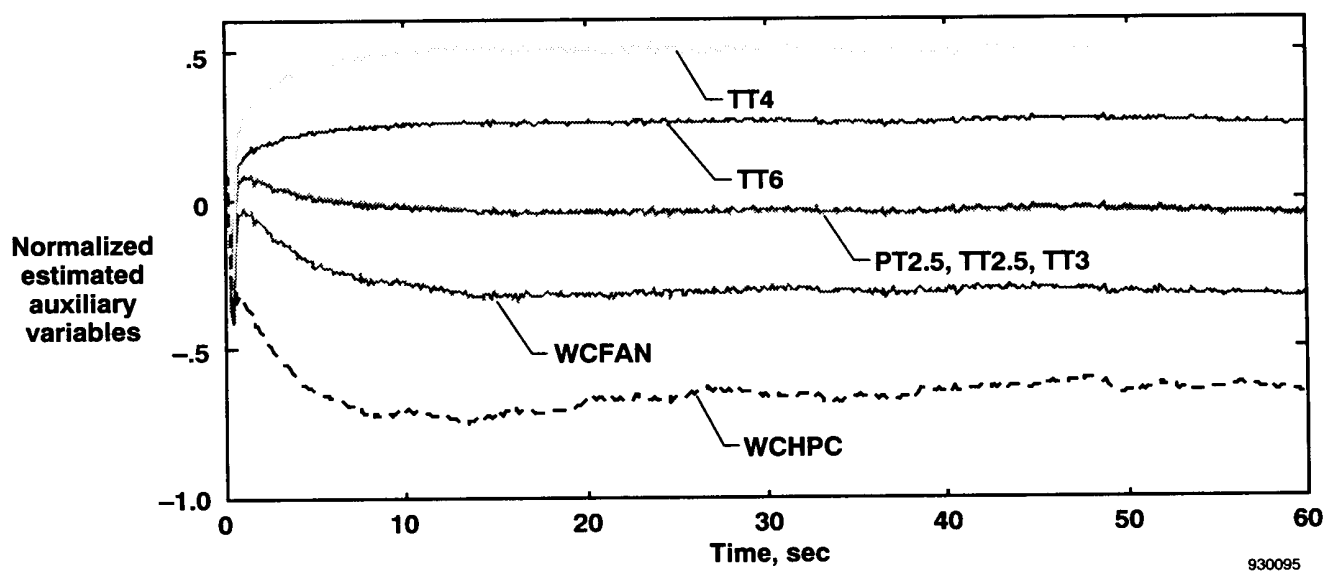(b) SSMLO approach.

Fig. 13 Normalized estimated EDPs.

30

(a) KF approach.

(b) SSMLO approach.

Fig. 14 Normalized estimated auxiliary variables.

31

REPORT DOCUMENTATION PAGE

Public reporting burden for this collection of information is estimated to average 1 hour per response, including the time for reviewing instructions, searching existing data sources, gathering and maintaining the data needed, and completing and reviewing the collection of information. Send comments regarding this burden estimate or any other aspect of this collection of information, including suggestions for reducing this burden, to Washington Headquarters Services, Directorate for Information Operations and Reports, 1215 Jefferson Davis Highway, Suite 1204, Arlington, VA 22202-4302, and to the Office of Management and Budget, Paperwork Reduction Project (0704-0188), Washington, DC 20503.

1. AGENCY USE ONLY (Leave blank)	2. REPORT DATE December 1993	3. REPORT TYPE AND DATES COVERED Technical Memorandum

4. TITLE AND SUBTITLE

On the Estimation Algorithm Used in Adaptive Performance Optimization of Turbofan Engines

6. AUTHOR(S)

Martín D. España and Glenn B. Gilyard

5. FUNDING NUMBERS

RTOP 533-02-39

7. PERFORMING ORGANIZATION NAME(S) AND ADDRESS(ES)

NASA Dryden Flight Research Facility
P.O. Box 273
Edwards, California 93523-0273

8. PERFORMING ORGANIZATION REPORT NUMBER

H-1908

9. SPONSORING/MONOTORING AGENCY NAME(S) AND ADDRESS(ES)

National Aeronautics and Space Administration
Washington, DC 20546-0001

10. SPONSORING/MONITORING AGENCY REPORT NUMBER

NASA TM-4551

11. SUPPLEMENTARY NOTES

Prepared as paper 93-1823 for the AIAA Joint Propulsion Conference, June 28–July 1, 1993, Monterey, CA.

12a. DISTRIBUTION/AVAILABILITY STATEMENT

Unclassified—Unlimited
Subject Category 07

12b. DISTRIBUTION CODE

13. ABSTRACT (Maximum 200 words)

The performance seeking control algorithm is designed to continuously optimize the performance of propulsion systems. The performance seeking control algorithm uses a nominal model of the propulsion system and estimates, in flight, the engine deviation parameters characterizing the engine deviations with respect to nominal conditions. In practice, because of measurement biases and/or model uncertainties, the estimated engine deviation parameters may not reflect the engine's actual off-nominal condition. This factor has a necessary impact on the overall performance seeking control scheme exacerbated by the open-loop character of the algorithm. In this report, the effects produced by unknown measurement biases over the estimation algorithm are evaluated. This evaluation allows for identification of the most critical measurements for application of the performance seeking control algorithm to an F100 engine. An equivalence relation between the biases and engine deviation parameters stems from an observability study; therefore, it is undecided whether the estimated engine deviation parameters represent the actual engine deviation or whether they simply reflect the measurement biases. A new algorithm, based on the engine's (steady-state) optimization model, is proposed and tested with flight data. When compared with previous Kalman filter schemes, based on local engine dynamic models, the new algorithm is easier to design and tune and it reduces the computational burden of the onboard computer.

14. SUBJECT TERMS

Adaptive optimization, Measurement biases influence, Parameter estimation, Performance seeking control, Propulsion systems

15. NUMBER OF PAGES
36

16. PRICE CODE
AO3

17. SECURITY CLASSIFICATION OF REPORT Unclassified	18. SECURITY CLASSIFICATION OF THIS PAGE Unclassified	19. SECURITY CLASSIFICATION OF ABSTRACT Unclassified	20. LIMITATION OF ABSTRACT Unlimited